



Measurements of friction, heat transfer, and mass transfer in a severely outgassing tube bank

B. Debusschere*, K. W. Ragland

Department of Mechanical Engineering, University of Wisconsin, Madison, WI 53706, U.S.A.

Received 27 June 1997; in final form 28 January 1998

Abstract

The influence of outgassing on the transport coefficients for flow through a staggered row tube bank was measured. Friction factors and heat and mass transfer coefficients were measured for $8000 < Re < 16000$ and blowing rates up to $v_0/U_x = 5 \times 10^{-3}$. Because of outgassing, heat and mass transfer coefficients reduced by as much as 70%. New blowing factors and correction functions were obtained that quantify the effect of outgassing on the transport coefficients.

© 1998 Elsevier Science Ltd. All rights reserved.

Nomenclature

A channel cross section
 c_p specific heat [$J\ kg^{-1}\ K^{-1}$]
 d diameter
 D diffusion coefficient
 f friction factor
 G mass flux = ρU [$kg\ m^{-2}\ s^{-1}$]
 h heat transfer coefficient
 h_m mass transfer coefficient
 k thermal conductivity
 \dot{m}'' mass flux [$kg\ m^{-2}\ s^{-1}$]
 n_{rows} number of rows in the tube bank
 p pressure
 P pressure coefficient
 Pr Prandtl number = $\mu c_p/k$
 q'' heat flux [$J\ m^{-2}\ s^{-1}$]
 Re Reynolds number = $\rho U_s d/\mu$
 Sc Schmidt number = μ/D
 St_h heat transfer Stanton number = h/Gc_p
 St_m mass transfer Stanton number = h_m/G
 T temperature
 U velocity in the main flow direction
 U_s superficial velocity = V/A
 v velocity normal to the tube surface
 V volumetric flow rate [$m^3\ s^{-1}$]
 x pitch of a tube bank

X mass concentration of H_2O [kg/kg mixture].

Greek symbols

β blowing factor
 μ dynamic viscosity
 ρ density
 ϕ correction function to account for outgassing
 ϕ angle.

Subscripts

a air
c in minimum free flow area
cp constant property
f friction
h heat transfer
l longitudinal
m mass transfer
s superficial
t transversal
w water
0 at surface
 ∞ in the free stream.

Superscript

0 value of the corresponding variable for the non-outgassing case.

1. Introduction

In many applications involving convective mass transfer, the mass transfer rates are relatively small such that

* Corresponding author.

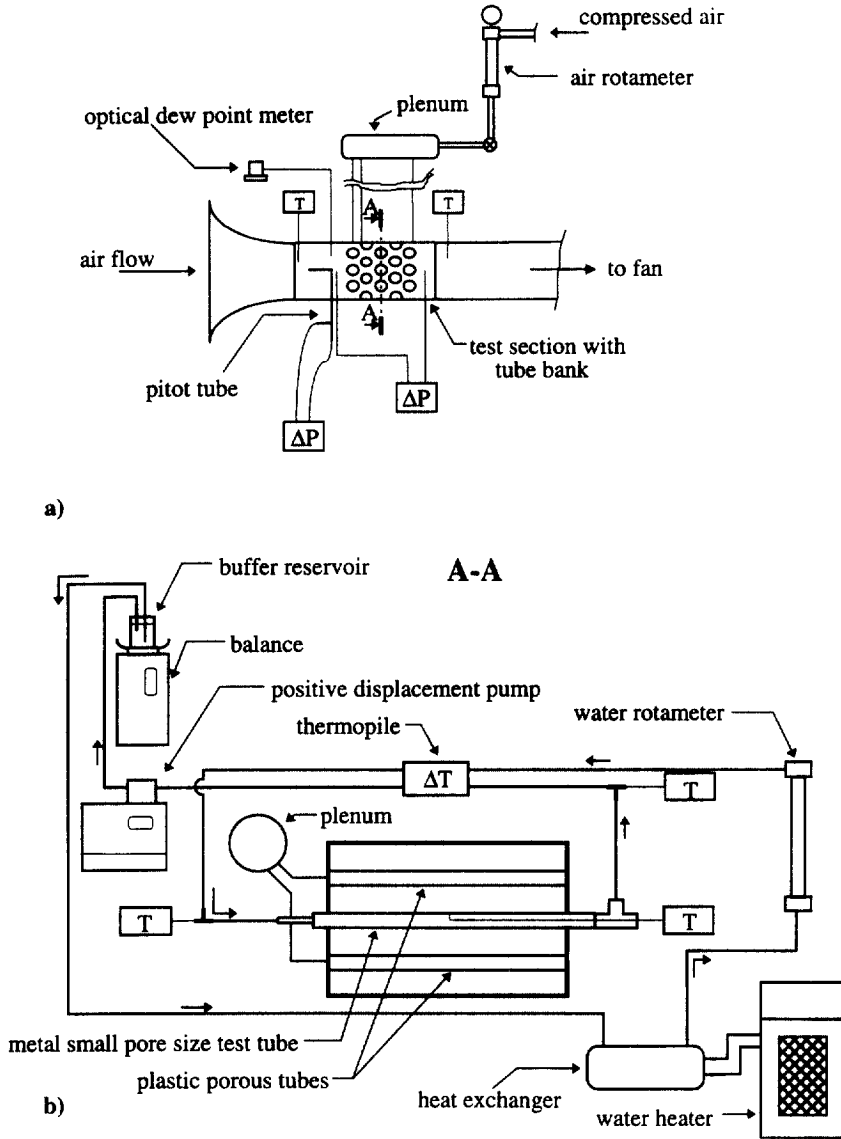


Fig. 2. Schematic of the test set-up. (a) All components relating to the air flow across the tubes in the test section and the air flow through the walls of the tubes. (b) Cross section A-A shows the water loop. The water circulates through the center porous tube where it evaporates.

an overall friction factor f , which is defined in this work as:

$$f = \frac{\Delta p}{n_{\text{rows}} \frac{\rho U_s^2}{2}} \tag{5}$$

The friction factor measurements (Fig. 3) extend the Reynolds number range in the data of Kays and London ([4], p. 215) from 3000 to 16 000. For our experiments, equation (5) yields the following correlation for the friction factors in a non-outgassing tube bank (see Fig. 3):

$$f = 39.0 Re^{-0.25} \quad \text{for } 3000 < Re < 16\,000. \tag{6}$$

When compressed air is blown through the pores of all tubes, the overall friction factor increases by up to 50% (Fig. 4). This overall friction factor is calculated from equation (5) using the superficial velocity U_s at the inlet of the test section. The Reynolds number is calculated at the inlet as well. The amount of outgassing is quantified by the blowing factor β_t , which is defined as:

$$\beta_t = \frac{\dot{m}''}{G_s} \tag{7}$$

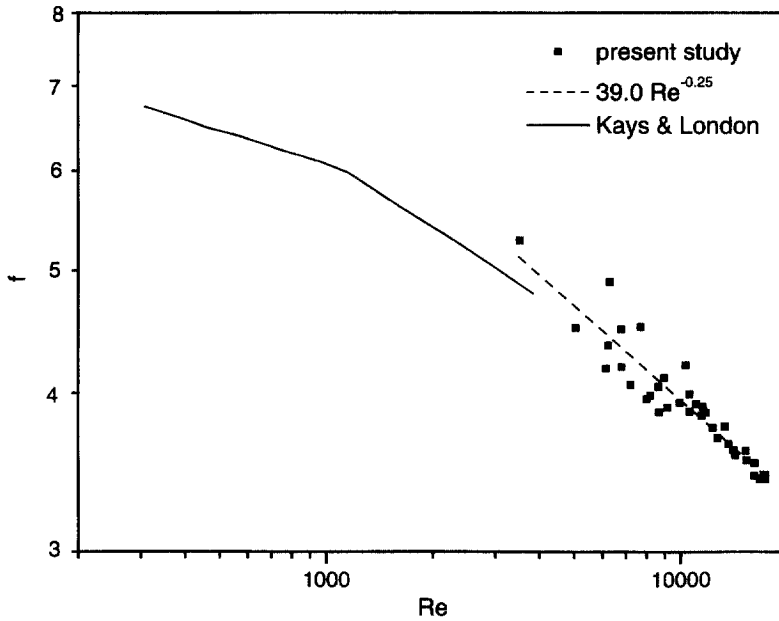


Fig. 3. Comparison of the friction factors measured in the present set up with the data of [4] (no outgassing).

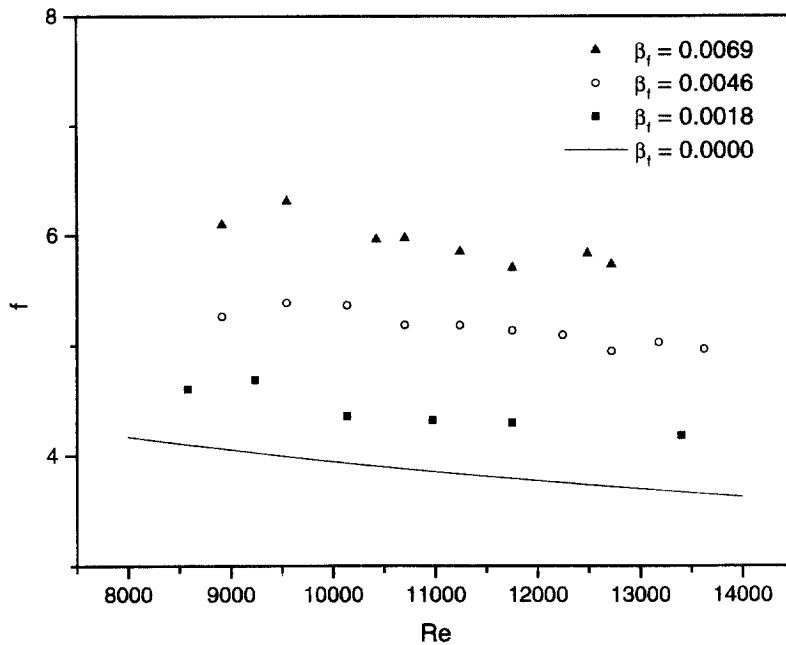


Fig. 4. Friction factors as a function of the inlet Reynolds number for various outgassing rates.

This is the ratio of the mass flux through the wall of the tubes to the mass flux in the minimum free flow area at the inlet of the tube bank (cross section B-B in Fig. 1). The outgassing apparently alters the boundary layer around the cylinders causing a higher pressure drop.

A more detailed picture of the effect of blowing on the boundary layer was obtained by measuring the static pressure around the perimeter of the center tube for various Reynolds numbers and blowing levels. This pressure distribution is a direct representation of the form drag

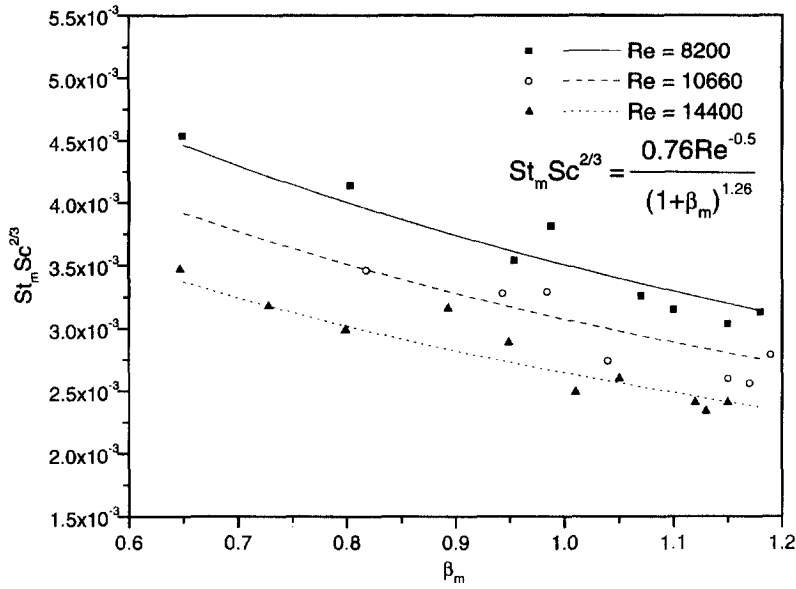


Fig. 8. $St_m Sc^{2/3}$ as a function of the blowing parameter β_m for various Reynolds numbers. The curves show the correlation to the test data.

blowing factor definitions are a modification of the definitions used by Kays and Crawford, who do not have the density ratio between air and water vapor in their blowing factors, equation (3) ([3], p. 501). Including this density ratio in the blowing factors better represents the physics of a boundary layer with non-uniform properties, which can be seen by expanding equation (11):

$$\beta_h = \frac{\dot{m}'' \rho_a}{G \rho_w} \frac{1}{St_h} = \frac{v_0 \rho_a c_{p,a} (T_0 - T_x)}{-k \left. \frac{\partial T}{\partial y} \right|_0}$$

$$= \frac{\text{convective transport}}{\text{molecular conduction}}$$

$$\beta_m = \frac{\dot{m}'' \rho_a}{G \rho_w} \frac{1}{St_m} = \frac{v_0 \rho_a (X_0 - X_x)}{-\rho D \left. \frac{\partial X}{\partial y} \right|_0}$$

$$= \frac{\text{convective transport}}{\text{molecular diffusion}} \tag{12}$$

Equation (12) shows that as the blowing factors get bigger, the convective transport within the boundary layer by the mass flux through the wall gets more important with respect to the regular molecular transport processes and the transport coefficients change correspondingly.

To find the effect of outgassing on heat and mass transfer processes in general, a correlation for the experimental data was used in the following form:

$$\frac{St}{St^0} = \varphi(\beta) \tag{13}$$

This assumes that the influence of the blowing is independent of the Reynolds number and fluid properties like Pr or Sc number. St^0 denotes the Stanton number that would be observed in a set-up with the same geometry and under the same conditions (i.e. same Re , Pr , Sc , ...) but with impermeable walls such that no outgassing occurs. However, data for St^0 for both heat and mass transfer could not be found in the literature for the geometry and Reynolds numbers studied. The direct measurement of St^0 with the present set-up was not feasible because of loss of accuracy at low evaporation rates. Therefore it was assumed that for the range of Reynolds numbers used, St^0 could be correlated as follows:

$$St_h^0 Pr^{2/3} = a_h Re^{b_h}$$

$$St_m^0 Sc^{2/3} = a_m Re^{b_m} \tag{14}$$

The form of equation (14) is frequently used for the correlation of heat and mass transfer data in geometries ranging from flat plates to single cylinders or tube banks in cross flow. The values for the parameter b range from about -0.4 to -0.53 ([2-4, 6] and [14] as cited in [15]). In the present study, the range of Reynolds numbers was not big enough to obtain an accurate value for the coefficient b by curve fitting to the data points. Therefore, a value of -0.5 was assumed for both b_h and b_m , which is a suitable value for the range of Reynolds numbers studied. For the function $\varphi(\beta)$, a form was chosen following [9]:

$$\varphi(\beta) = \frac{1}{(1 + \beta)^c} \tag{15}$$

This equation satisfies the condition that $\varphi(0) = 1$.

After substituting equations (14) and (15) into (13) and performing a least squares fit to all available data points, the following correlations were obtained for St_h and St_m :

$$St_h Pr^{2/3} = \frac{a_h Re^{-0.5}}{(1 + \beta_h)^{c_h}} \quad \begin{cases} a_h = 1.54 \\ c_h = 2.14 \end{cases}$$

$$St_m Sc^{2/3} = \frac{a_m Re^{-0.5}}{(1 + \beta_m)^{c_m}} \quad \begin{cases} a_m = 0.76 \\ c_m = 1.26 \end{cases} \quad (16)$$

Figures 7–8 show the graphical representation of these correlations for three different Reynolds numbers. The uncertainties on a and c are less than 5% for both correlations. Combining equations (13)–(15) with equation (16), the following functions $\varphi(\beta)$ resulted:

$$\frac{St_h}{St_h^0} = \varphi_h(\beta_h) = \frac{1}{(1 + \beta_h)^{2.14}} \quad (0.45 < \beta_h < 1.2)$$

$$\frac{St_m}{St_m^0} = \varphi_m(\beta_m) = \frac{1}{(1 + \beta_m)^{1.26}} \quad (0.6 < \beta_m < 1.2) \quad (17)$$

In Figs 9–10, the curves $\varphi(\beta)$ as given by equation (17) for heat and mass transfer, respectively, are compared to the data points divided by $a \cdot Re^{-0.5}$. These figures show a good agreement between equations (17) and the data divided by $a \cdot Re^{-0.5}$ (the correlation coefficient between the curve and the data points is about 0.94 in both figures). Moreover, there is no Reynolds number dependency left in the data after dividing by $a \cdot Re^{-0.5}$. This indicates that the functions φ are indeed dependent on the blowing factors β only and that the exponent of -0.5

for the Reynolds number is appropriate. Figures 9–10 show a significant decrease in the surface transport coefficients due to the outgassing. Reductions up to 70% have been measured, which affects the design of heat and mass transfer processes involving high outgassing rates. The functions φ are correction functions to account for the effect of outgassing. When the transport coefficients for the non-blowing case are known, the ones for the outgassing case can be obtained through multiplication by the functions $\varphi(\beta)$.

4. Conclusions

Measurements of friction coefficients and heat and mass transfer coefficients have been performed for a staggered tube bank with outgassing cylinders in cross flow. Due to outgassing, the overall friction factor increased by up to 50%. For heat and mass transfer coefficients, however, reductions up to 70% were measured due to outgassing. These large reductions in heat and mass transfer coefficients and the increase in pressure drop affect the design of equipment with high outgassing conditions.

The influence of outgassing on heat and mass transfer coefficients was correlated using a new set of non-dimensional blowing factors β , equation (11), and a new form for the correction functions $\varphi(\beta)$, equation (17). The blowing factors are able to quantify blowing in boundary layers with non-uniform fluid properties since they rep-

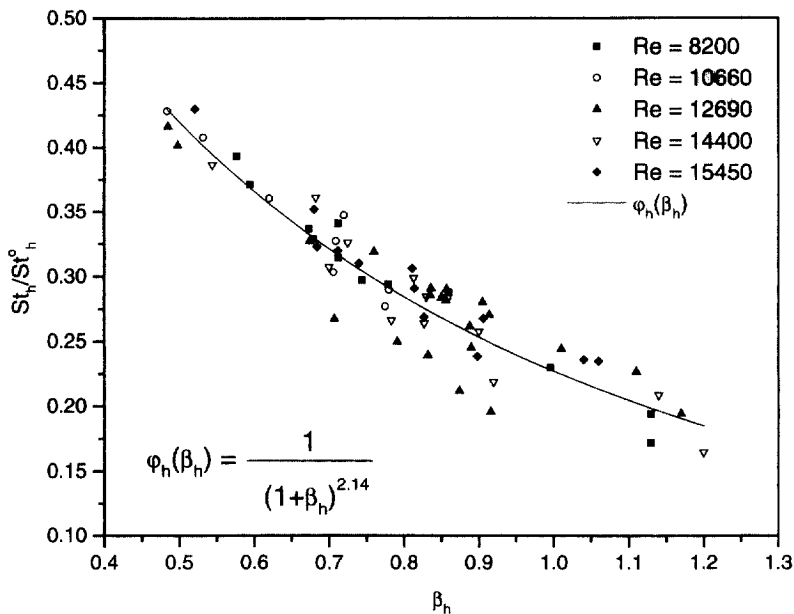


Fig. 9. Comparison of the correction function $\varphi(\beta_h)$ to the data points.

